iJET EXPLORE International Journal of Engineering & Technology
CENTRE OF PROFESSIONAL RESEARCH PUBLICATIONS
ISSN 2049-3444

International Journal of Engineering and Technology Volume 2 No. 12, December, 2012

Weldability of Recycled Steel Bars in Uganda

Senfuka C., Kirabira J.B., Byauhanga J.K.
Kyambogo University, Kampala District, Uganda

ABSTRACT

The metallurgical reliability of welded recycled steel made in Uganda has been studied through the examination of manual metal arc weldments of steel samples of 0.27%C and less using the dye penetrant flaw detection method, micro-hardness plots and spark spectromentry. This method was selected to ensure reproducibility by taking repeated readings on the same sample since it is largely non-destructive. About thirteen percent of the samples exhibited post-weld cracks. Of these, 3% of the samples yielded hot cracks while the other 10% showed typical hydrogen assisted cracks. The cracking sensitivity has been attributed to the presence of large numbers and quantities of residual elements rather than high carbon content in particular. This resulted from the predominantly recycled production mode in the country. The use of more elaborate refining methods and the exploitation of virgin iron resources have been recommended. Pre- and post-heating techniques have been advised whenever weld cracking threatens.

Keywords: *Steel welding, Residual elements, Hydrogen cracking, Ductility, Recycled steel.*

1. INTRODUCTION

The relative ease with which a metal or alloy can be joined by fusion is termed weldability. It encompasses the metallurgical compatibility of the metal with a specific welding process, its ability to be joined with mechanical soundness, and the capacity of the resulting weld to perform satisfactorily under the intended service conditions (Jyoti et al., 2012).

The engineering world has very often needed to make all kinds of joints in order to produce useful items from bar stock and other forms of raw materials. The ease with which most commercial metals can be joined using fusion welding has made them particularly versatile in the manufacture of fabricated items. The major limitation of welded joints is the frequent tendency to welding defects which include any flaw or discontinuities that compromise the usefulness of the finished weldment.

Many welding faults such as lack of fusion, lack of penetration, porosity, undercut, arc strikes, and others are associated with poor workmanship while discontinuities such as laminations, delaminations, seams and laps result from rolling operations in the steel making process.

The most insidious discontinuities however, are those that cause brittle cracking of metallurgical origin. Such brittle failures are characterized by intergranular, interdendritic, cleavage or quasi-cleavage and micro-void coalescence modes of fracture, occurring at stress levels well below the ultimate stress of either weld or base metal and at reduced levels of ductility. Many of these can act as stress concentration sites to reduce weld joint strength and promote cracking and fatigue failure. Steel in Uganda being entirely of the recycled origin, tends to be of unpredictable weldability due to the effect of tramp elements that introduce many of these imperfections.

Cracks in any form or size are usually unacceptable and are considered most detrimental to the performance and longevity of the weld. A crack, by its nature, is sharp at its extremities and consequently acts as a stress concentration site. The stress concentration effect of a crack is greater than that of most other discontinuities. Cracks have a tendency to propagate and can contribute to extended weld failure if subjected to stress in service.

Weld cracking is the result of solidification, cooling and the stress due to weld shrinkage formed when a critical tensile strain specific to the alloy is exceeded and occurs as the weld metal in the fusion zone cools due to the fact that the resulting contraction is restricted, giving rise to two opposing forces; the stress caused by the shrinkage of the metal and the surrounding rigidity of the base material (Prokhorov, 1956). Strains in higher yield strength filler and base metals thus give rise to higher stresses.

Physical processes that occur due to the interaction of the heat source with the metal during welding which include re-melting, heat and fluid flow, vaporization, dissolution of gasses, solidification, subsequent solid-state transformation, stresses and distortion further complicate microstructural development in the fusion zone. These processes and their interactions profoundly affect weld pool solidification and microstructure, often leading to unpredictable physical features closely linked to the formation of cracks and other discontinuities (Bernasovský, 2009).

Unlike service related weld failure, welding cracks occur close to the time of fabrication. Cracks can occur in the weld metal or in the parent material and can be hot or cold cracks. Hot cracks are usually intergranular along primary austenite boundaries and therefore occur at elevated temperatures. These temperatures are known to be between liquidus and solidus during which range the weld bead is mushy. They form in the weld as tensile stresses and strains build behind the moving weld pool as a result of solidification shrinkage and thermal contraction as influenced by welding parameters and the degree of restraint (Thomas, 2011).

Hot cracks can be of transverse, longitudinal and crater types. Transverse weld metal cracks are perpendicular to the direction of the weld and are more common in welds that have a high degree of restraint. In transverse cracking, the weld is higher strength than the base metal. As the weld bead shrinks longitudinally, the surrounding metal resists in compression, restricting the required shrinkage. In this way the weld develops longitudinal stresses which facilitate cracking in the transverse direction (Carl, 2011).

Longitudinal weld cracks (Fig.2b) travel in the same direction as the weld and are often confined to the center of the weld. More often than not, these are segregation induced, and are formed in the centerline of the weld bead resulting from base metal contaminant pickup in which low melting point constituents like phosphorus, sulphur, zinc and copper compounds usually forced to the centre of the bead, solidify last. These give rise to a failure front since they tend to form a low strength zone at the weld centerline. They often limit the usable welding amperage to minimize penetration and the subsequent elemental contamination (Omar et. al,. 1999). A similar but not identical source of cracks is the existence of large temperature ranges between liquidus and solidus as in the case of iron and many of the tramp elements in steel (Fig.1). Tensile stresses due to shrinkage tend to prevail during the liquidus to solidus temperature range and pull the base metal ends apart before the actual solidification of the weld, leading to solidification cracking (Devletian, 2008).

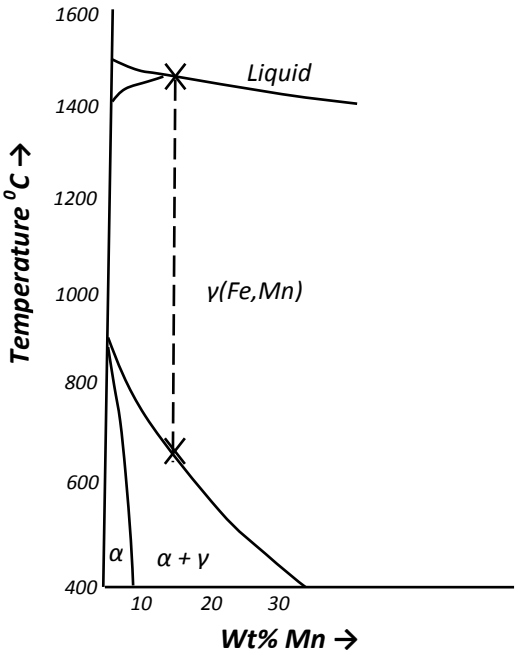

Fig.1: Iron rich end of the Fe-Mn equil. diagram

Crater cracks can be formed by any abrupt weld termination if a crater is left unfilled within the weld metal (Fig.2c). These cracks are usually star shaped and initially only extend to the edge of the crater although they can propagate into the more serious longitudinal weld cracks.

Cold cracks (Fig.2a) on the other hand normally occur in the heat affected zone hours or even days after the weld has cooled to room temperature and may propagate both intergranular and transgranularly (Joy, 2009). They are normally hydrogen related. They are caused by the combined effects of low ductility of the weld, residual stress and diffusible hydrogen in the weld. The ductility of a weld is a function of the carbon equivalent and the cooling speed after solidification (Schlatter, 2012). Residual stresses in the weld are dependent on edge preparation and weld design and tend to be larger than

expected if it contains discontinuities such as incomplete fusion, inappropriate joint penetration, overlap, undercut, slag inclusions porosity etc. (Cary et al., 2005). The source of diffusible hydrogen in a weld is mainly moisture and organic compounds which may be in the base steel, in the electrode, in the shielding material or in the atmosphere (Albert et al., 2003).

Fig. 2(a): Cold crack

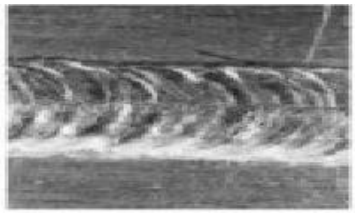

Fig. 2(b): Hot Longitudinal crack

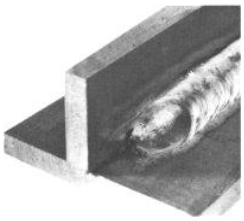

Fig.2(c) Crater crack

In this study, a relationship is established between the high levels of tramp elements, not necessarily carbon; in the Uganda recycled steel and its occasional welding deficiencies in order to establish the metallurgical reliability of the steel.

2. MATERIALS AND METHODS

Thirty pieces of 10mm steel square bars were randomly selected from steel plants in three different locations in the country. Two 150mm lengths were cut from each piece. The cut of pieces were prepared for V-groove flat position welding and designed to have more width than depth as shown in Fig.3. Single pass butt welds were made with 4mm diameter manual metal arc welding (MMA) rods (E6013) at 4mm per minute at 198 Amps, 100 volts setting. The samples were left to cool in still air and examined for cracks after 24 hours.

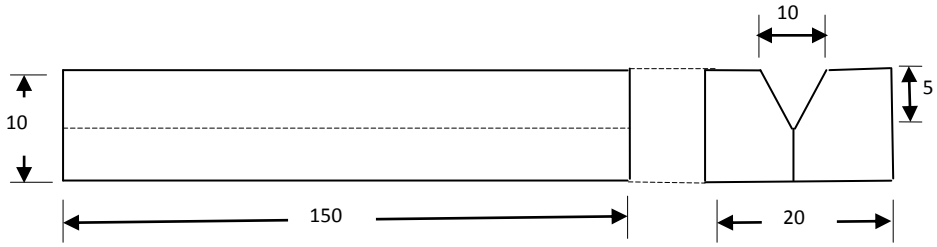

Fig.3: Edge preparation for welded samples

The weld bead was subsequently ground down with a surface grinder and micro-finished. The surfaces were cleaned with a petroleum distillate, treated with a red dye penetrant and later with calcium carbonate suspension in propanol/acetone as developer every after 48 hours for seven days. Transverse micro-hardness readings were taken with a Super Rockwell Duplex 713-SR hardness tester using a 1/16" ball across the face of the selected samples and hardness was plotted against transverse displacement.

The chemical composition of the four samples PV5, PV8, PV19 and PV26 which showed detectable cracks was also determined with a *SPECTROL AB* spark spectrometer.

Their Chromium equivalents were calculated as:

$$Cr_{eq} = Cr + 2Si + 1.5Mo + 5V + 5.5Al + 1.75Nb + 1.5Ti + 0.75W \quad (1)$$

while the Nickel equivalents were determined as:

$$Ni_{Eq} = Ni + Co + 0.5Mn + 0.3Cu + 30C \ (2) \ \text{(Antonio, 2009).}$$

The corresponding carbon equivalents have been calculated as:

$$C_{eq} = C + A(C) * \{Si/24 + Mn/6 + Cu/15 + Ni/20 + (Cr + Nb + V + Mo)/5 + 5B\} \quad (3)$$

where:

$$A(C) = 0.75 + 0.25tanh\{20(C - 0.12)\} \text{ (Yurioka et al., 1985).}$$

3. RESULTS

Out of the thirty samples welded and tested, four showed evidence of weld induced cracking. Fig. 5 shows sample PV5 with a typical centerline crack while Fig. 4 shows a HAZ crack after micro-finishing and treatment with die penetrant and developer.

The micro-hardness graphing across the face of the samples PV5 and PV19 is shown in Fig. 6. The hardness value at the centre of PV5 gradually drops ten HRb units below that of the base metal in response to the lower carbon equivalent of the filler rod (See Table 3) in the center in comparison to the edges. The final five units drop in hardness is in the center of the sample, showing the position of the crack.

In the case of PV19, the face hardness plot indicates the expected reduction in hardness in the weld fusion zone but suddenly drops 30 HRb units towards the right edge of the sample. The crack is located outside the weld and is well inside the parent metal.

The chemical composition of the four samples which developed cracks are as in Table 1. The four samples have carbon content levels falling in the range $0.22 \leq \% \leq 0.27$. The Manganese content is also medium. Worth noting is the presence of Boron at $0.002 \leq \% \leq 0.004$.

The Chromium, Nickel and Carbon equivalents were as in Table 2 as determined by equations 1, 2 and 3.

Table 1: Chemical Comp. %wt

S'ple	%C	%Cu	%B	%N	%C	%M	%M	%V	%Si	%N	%Ti	%A	%	%C
PV5	0.24	0.364	0.004	0.06	0.54	0.48	0.11	0.00	0.06	0.03	0.00	0.03	0.0	0.00
PV8	0.25	0.217	0.003	0.05	0.25	0.52	0.11	0.00	0.05	0.03	0.00	0.02	0.0	0.00
PV19	0.27	0.321	0.004	0.10	0.15	0.58	0.01	0.00	0.24	0.00	0.00	0.03	0.0	0.00
PV26	0.22	0.354	0.002	0.06	0.37	0.49	0.11	0.00	0.05	0.03	0.00	0.03	0.0	0.00

Table 2: Equivalents

S'ple	Ni_{eq}	Cr_{eq}	C_{eq}
PV5	7.62	1.08	0.54
PV8	7.89	0.71	0.49
PV19	8.59	0.89	0.49
PV26	7.02	0.93	0.48

Table 3: Deposition metal composition

Element	C	Mn	Si	S	P
%Comp.	0.12	0.05	0.35	0.035	0.04

Fig.4: Centerline crack, PV5

Fig. 5: Cold cracking, PV 19

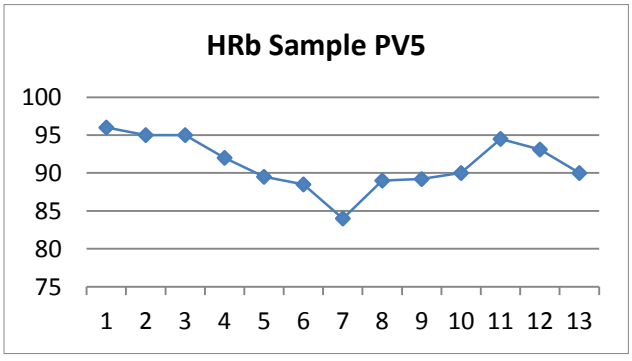

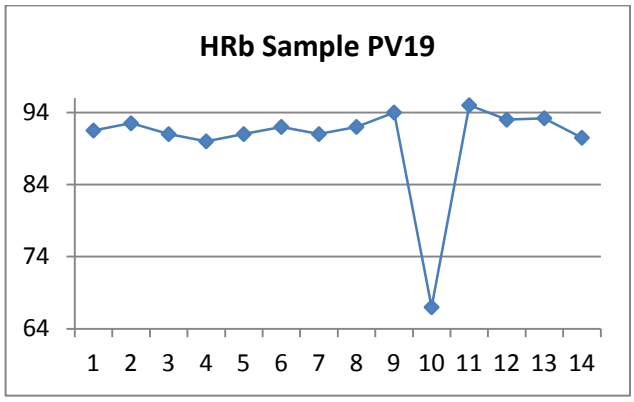

Fig.6: Micro-hardness plot for PV5 and PV19

4. DISCUSSION

The gradual drop in micro surface hardness of sample PV5 is the expected result of the lower tensile strength of the filler metal, being 330Mpa, reducing gradually due to penetration and dilution between stronger ($\square_u$=498Mpa), higher carbon equivalent base metal and the filler rod (Table 2 and 3). The additional drop just before the crack indicates that the centerline crack is related to the reduced hardness of the material around the crack. This actually shows that the crack is the result of solidification cracking derived from the accumulation of low melting temperature, softer material during the solidification process towards the center of the fusion zone, providing the weaker front that gave way due to tensile stress created in the weld by the solidification process and resulting contraction.

Hot cracking is also associated with the presence of liquid films along grain boundaries or elsewhere in the structure. The existence of a large temperature range between liquidus and solidus (Fig.1) as in the case of low carbon steel with manganese(see table 1) is a factor in the generation of the solidification cracks since the solidification stresses tend to have time to pull the base metal ends before the actual solidification of the weld. Weld solidification cracking occurs during the final stages of solidification when tensile shrinkage stress accumulates as liquid films still persist along solidification grain boundaries in the structure. If the imposed shrinkage strain exceeds the inherent ductility of the solidifying weld metal, cracking will occur (Joel, 2011). The brittle temperature range (BTR), the temperature range over which this occurs, is represented by a drop in ductility between the liquidus and solidus temperature, where the width (temperature) and depth (ductility) of the BTR can be used to assess susceptibility to weld solidification cracking. (John, 2005). It has been argued that alloys with a large BTR will be exposed to a greater accumulated strain during cooling and thus exceed the ductility limit (Carl et. al., 2011). This tendency has been expressed by the solidification cracking factor L_t given as:

$$L_t = 70(C - Si/12 - Mn/9 + 3P + 4S + Ni/23 + Cr/35 + Mo/70) \ldots\ldots\ldots\ldots\ldots\ldots \quad (1)$$ (Matsuda, F., 1990).

The entities in this equation indicate the dependence of solidification cracking on silicon, manganese, nickel and molybdenum which are also key residual elements in steel, reminiscent of the recycling process.

This would be accentuated by the presence of low-melting point products enriched impurities such as sulfur and phosphorus and probably tin originating from the base metal which tend to solidify last (Devletian, 2008). The distribution of these and other solutes during weld pool solidification is an important phenomenon resulting in segregation that can significantly affect weldability, microstructure, and properties (David, 2003).

On the other hand, Figure 5 shows the crack detection image of P19. This crack was identified in the base metal three days after weld solidification. This is the usual position for cold cracks. Although cold cracking could have taken place either in the weld metal or the HAZ depending on which is more susceptible, the peak hardness and strength values in the HAZ are greater than those of the weld metal in sample PV19 according to micro-hardness plot in Fig.6. So, a typical hydrogen crack had to occur in the HAZ. The presence of crack promoting elements like Boron, chromium etc (equation 2) in the HAZ makes this more likely. In the empirical relationship for carbon equivalent in equation 2 (Yurioka et al., 1985), the effect of carbon and boron is strongly shown to favor welding crack formation. These elements tend to elevate the carbon equivalent value and the critical cooling rate which in turn determine the crack forming susceptibility of the microstructure and thus increase the hydrogen cracking tendency.

The boron content in PV5 and PV19 at 0.004 is relatively higher than the rest of the samples tested (Table1).

There have also been suggestions of effects of pre-existence of defects like inclusions, minor phase particles, microscopic cracks, and other discontinuities acting as initiation sites in hydrogen initiated cracking (Devletian, 2008). The presence of large amounts of tramp elements in Ugandan recycled steel and specifically the four samples in Table 1 invariably leads to multitudes of minor phase particles in their different forms such as MnS, Cr_7C_3, WC etc. This also includes products of deoxidation like Al_2O_3.

It has been argued that during the welding process, while the metal is still in molten state, molecular hydrogen